Thesis Title

A subtitle of your thesis

Author name

Thesis submitted for the degree of
Master in Master's Program Name <change at main.tex>
60 credits

Department Name <change at main.tex>
Faculty name <change in duoforside.tex>

UNIVERSITY OF OSLO

Spring 2022

Thesis Title

A subtitle of your thesis

Author name

Thesis Title

http://www.duo.uio.no/

Printed: Reprosentralen, University of Oslo

Abstract

Contents

List of Figures

List of Tables

Preface

Chapter 1

Introduction

some introduction on the importance of discovering new materials and alloying.
Need something on thermoelectricity related to both the band gap and high-entropy alloys.

High-entropy alloys is a novel class of materials based on alloying multiple components, as opposed to the more traditional binary alloys. This results in an unprecedented opportunity for discovery of new materials with a superior degree of tuning for specific properties and applications. Recent research on high-entropy alloys have resulted in materials with exceedingly strong mechanical properties such as strength, corrosion and temperature resistance, etc **find references**. Meanwhile, the functional properties of high-entropy alloys is vastly unexplored. In this study, we attempt to broaden the knowledge of this field, the precise formulation of this thesis would be an exploration on the possibilities of semiconducting high-entropy alloys.

A key motivation of this thesis is the ability to perform such a broad study of complex materials in light of the advances in material informatics and computational methods. In this project, we will employ Ab initio methods backed by density functional theory on top-of the line supercomputers and software. 20 years ago, at the breaking point of these methods, this study would have been significantly narrower and less detailed firstly, but secondly would have totaled ... amount of CPU hours to complete (**Calculate this number**). In the addition to the development in computational power, is also the progress of modeling materials, specifically we will apply a method called Special Quasi-random Structures (SQS) to model high-entropy alloys or generally computationally complex structures. Together with the open landscape of high-entropy alloys described above, these factors produce a relevant study in the direction of applying modern computational methods to progress the research of a novel material class and point to promising directions for future research.

In specifics, this thesis revolve around the electrical properties of high-entropy alloys, mainly the band gap as this is the key indicator for a semiconducting material and it's applicability. Semiconductors are the building blocks in many different applications in today's world, ranging

from optical and electrical devices, to renewable energy sources such as solar and thermoelectricity. Given the economic and sustainable factors concerning silicon, in addition to its role in relevant applications such as microelectronics and solar power. Silicon emerges as a natural selection to build our alloys around. Furthermore, the development and research on both high entropy alloys and metal silcides have been heavily centered around 3d transition metals. Keeping in line with the economic and environmental factors, we will continue this direction by focusing on high entropy stabilized sustainable and economic 3d metal silicides **Not happy with this writing**. Throughout the study we will analyze a great number of permutations of 3d silicides, from different initial metal silicides such as $CrSi_2$, $FeSi_2$, $MnSi_{1.75}$, Fe_2Si, each with distinct properties relating to the band gap, crystal structure and metal to silicon ratio. In addition, the permutations include numerous metal distributions and elements within the 3d-group of metals. Examples are Co, Cr, Fe, Mn, and Ni.

Given a background in high-entropy alloys, one could ask if this study is truly sensible. In the later sections we will cover the details of this field, and it quickly become clear that the materials investigated in this study does not fall under the precise definition of high-entropy alloys, nor do we intend to explore the properties and factors relating to high-entropy stabilized alloys such as the configurational entropy, phase stability and finite temperature studies. However this study is motivated from the discovery of these materials and promising properties, and venture into a more hypothetical space of materials, enabled by the computational methods available to study the potential properties of such materials. On the other hand, very recent studies **Mari, and other HEA silicide study** have experimentally synthesized high-entropy disilicides, thus in some way justifying the direction of this project.

We begin this project by reviewing key concepts of solid-state physics for readers lacking a background in materials science, and an introduction to the base 3d silicides of the experimental work. Later follows a theoretic walk-through of the relevant concepts of this thesis, these topics include high-entropy alloys, special quasi-random structures, and density functional theory. Next we shine light on the implementation of DFT in this project, and other computational details required to reproduce the results in this thesis, such as the use of the Vienna Ab Initio Simulation Package (VASP) and implementation of SQS. Finally we present the results of our study, these include the band gap and electronic properties of various structures and the success and challenges of the computational methods applied throughout the study.

Part I

Theory

Part II

Methodology and Implementation

Part III

Results and Discussion

Chapter 8

Permutations of $(CrFeMnNi)Si_2$

Up until this point we have looked in detail at the high-entropy silicide $(CrFeMnNi)Si_2$ and associated SQSs. However these structures are just the center of a larger quasi-ternary phase diagram consisting of the different possible distributions of elements Thus there exists many other compositions of this particular high-entropy silicide. In this section, we aim to expand our search of this diagram by generating SQSs of the 48 atom model slightly away from equimolar distribution of 3d elements. In table (bellow) we list the mean total energy and magnetic moment per atom with standard deviation and the enthalpy of formation of 4 compositions of the $(CrFeMnNi)Si_2$ alloy. Ideally they would differ only by one element, but the TDEP implementation insist in also reducing Nickel to stay consistent with the 48 atom supercell.

Composition	Toten (eV)		Mag (μ_B)		ΔH (eV)
	mean	std	mean	std	mean
$Cr_3Fe_3Mn_7Ni_3Si_{32}$	- 6.6947	0.0040	0.1375	0.0186	-11.9586
$Cr_5Fe_5Mn_3Ni_3Si_{32}$	- 6.6705	0.0030	0.1127	0.0223	-11.1991
$Cr_5Fe_3Mn_5Ni_3Si_{32}$	- 6.6852	0.0041	0.1375	0.0456	-10.5200
$Cr_3Fe_5Mn_5Ni_3Si_{32}$	- 6.6801	0.0036	0.0937	0.0209	-12.6426
$Cr_3Fe_3Mn_3Ni_7Si_{32}$	- 6.3921	0.0078	0.0159	0.0101	-10.9614

Table 8.1: Summary composition diagram

The first result of table .. we make notice of is that the stability, as evaluated by the enthalpy of formation can be increased beyond the eqvimolar composition. This is accomplished in two distinct permutations, one with increments to manganese relative to the other TM, and the other by reduction of chromium. Compared to the equimolar system, the magnetic moment of these compositions show a greater variation between SQSs, as indicated by the standard deviation. Typically the most stable

SQS lie around the mean value of the set. The large magnetic moment of the manganese rich permutation and the low magnetic moment in the chromium poor permutation is very much in line with the observations made in the previous section. Recalling that in the magnetic moment in the equimolar composition was largely attributed to manganese and chromium atoms in the lattice. Thus increments to manganese or reduction of chromium would following impact the magnetic moment as seen. Following the composition $Cr_5Fe_3Mn_5Ni_3Si_{32}$ where the nonmagnetic elements are reduced and the magnetic elements are increased, the final magnetic moment is among the highest of the bunch equally magnetic.

In table 8.2 we list the respective band gaps of the different compositions calculated with the PBE functional. Only the GGA functional was applied in this case because the motivation is primarily to compare the results to the parent equimolar composition and thus including 3 times as many results to calculate and analyze unnecessarily complicate the process. Thus we base this comparison between the PBE results of the new compositions to the PBE band gaps of the equimolar compound. In these compositions we find strong indication of a half-metal with less frequent SQSs with a band gap in the spin down channel than the equimolar compound. In the spin up channel on the other hand several compositions show very similar values to the equimolar composition. Between the different compositions particularly those rich in manganese provide very encouraging results and compositions poor in Mn less so. In terms of the stability we a very encouraging results of both the $Cr_3Fe_3Mn_7Ni_3Si_{32}$ and $Cr_3Fe_5Mn_5Ni_3Si_{32}$ compositions, where the most promising properties is attributed to the utmost stable configurations. in $Cr_3Fe_5Mn_5Ni_3Si_{32}$ the most stable SQS (D) is a semiconductor with a band gap around 0.1 eV.

Below in figure 8.1 we plot the projected density of states around E_F of the fist four compositions of table 8.2. Note that away from the Fermi energy the projected density of states is analogous to the parent equimolar composition. The below figures is based on the most stable SQS in each permutation, as will the analysis. Hence the features of these figures can be subject to the uniqueness of that particular SQS rather than a distinct feature of the exact composition, but as stated previously the most stable configuration provide the most likely properties of the composition within the scope of this project.

Composition	SQS	$E_G^{\text{up, eigen}}(0.5)$ (eV)	$E_G^{\text{dw, eigen}}(0.5)$ (eV)	$E_G^{\text{tot, eigen}}(0.5, 0.5)$ (eV)
$Cr_3Fe_3Mn_7Ni_3Si_{32}$	A	0.3390	0	0
	B	0.4745	0	0
	C	0.1342	0	0
	D	0.1950	0.0063	0.0063
	E	0.4211	0	0
$Cr_5Fe_5Mn_3Ni_3Si_{32}$	A	*0.003*	0	0
	C	*0.21*	0	0
	D	0.0674	0.0413	0.0372
	E	*0.362*	0	0
$Cr_5Fe_3Mn_5Ni_3Si_{32}$	**A**	0.2082	0	0
	B	0.4053	0	0
	C	0.4659	0	0
	D	0.0843	0.0121	0.0121
	E	0.3008	0	0
$Cr_3Fe_5Mn_5Ni_3Si_{32}$	A	0.3922	0	0
	C	0.1285	0	0
	D	0.2595	0.1004	0.1004
	E	0.3591	0.1003	0.0848
Cr3Fe3Mn3Ni7Si32	A	0	0	0
	B	0	0	0
	C	0	0	0
	D	0	0	0
	E	*0.04*	0	0

Table 8.2: Band gaps of various compositions of $(CrFeMnNi)Si_2$. Most stable SQS of a set is highlighted in bold text, defect band gap are listed in cursive. Some SQSs were excluded from the table due to unsuccessful calculations.

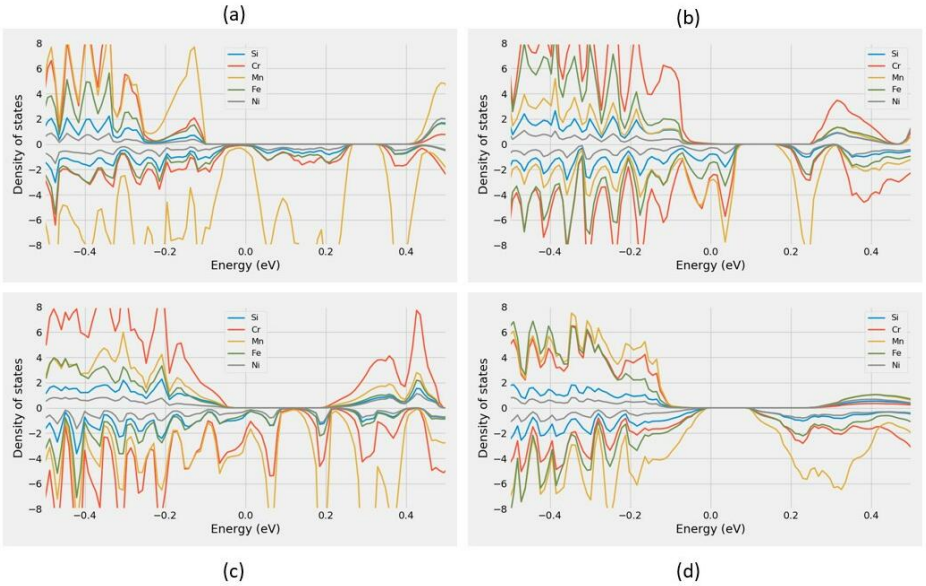

Figure 8.1: Projected density of states of (a) $Cr_3Fe_3Mn_7Ni_3Si_{32}$ (SQS B), (b) $Cr_5Fe_5Mn_3Ni_3Si_{32}$ (SQS C), (c) $Cr_5Fe_3Mn_5Ni_3Si_{32}$ (SQS A), (d) $Cr_3Fe_5Mn_5Ni_3Si_{32}$ (SQS D)

With that said, the plotted PDOSs in figure 7.1 is in good agreement with the listed values in table 7.2. $Cr_3Fe_3Mn_7Ni_3Si_{32}$ (7.1 a) and $Cr_5Fe_3Mn_5Ni_3Si_{32}$ (7.1 c) both indicate a sizable spin up band gap, further figure (7.1 d) point to a total band gap around 0.1 eV for SQS D of $Cr_3Fe_5Mn_5Ni_3Si_{32}$. On the other hand we find dissimilarity between the density of $Cr_5Fe_5Mn_3Ni_3Si_{32}$ SQS C and the eigenvalue band gap listed in table 7.2. In figure 7.1 d we find a range of forbidden energies slightly above the Fermi energy, and very small values in spin up at the Fermi energy. Similar to what we experienced in the 192 atom SQS in section 7.4, the eigenvalues report a finite band despite of defect states. Therefore the density of states is not completely zero at E_F.

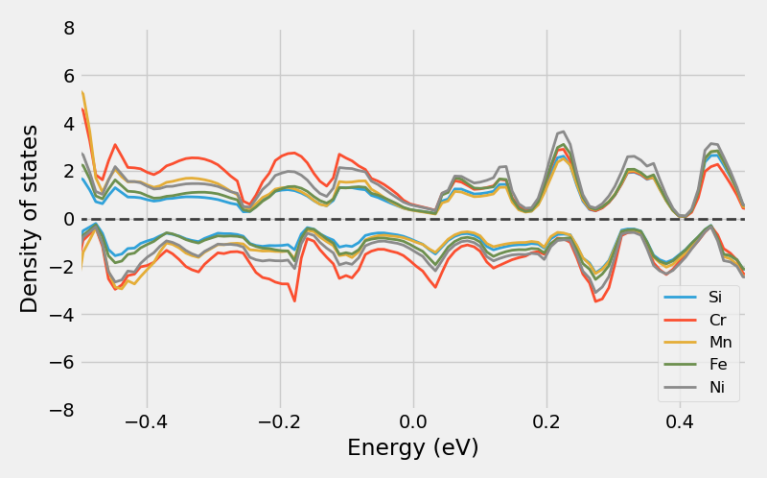

Figure 8.2: Projected density of states of $Cr_3Fe_3Mn_3Ni_7Si_{32}$ around E_F

In figure 8.6 we saw that electrons from manganese atoms in particular was a key contributor as to why the spin down channel of (CrFeMnNi)Si_2 was metallic in the stable supercell D. This is also largely the case in the permutations shown above in figure 8.12. The proportion of manganese atoms in the alloy seems to offer a very positive effect on the band gap in spin up, but is often detrimental to spin down. This is seen in figure 8.12 (a) and (c) for $Cr_3Fe_3Mn_7Ni_3Si_{32}$ and $Cr_5Fe_3Mn_5Ni_3Si_{32}$ respectively, that both contain increased amounts of manganese. By reducing the number of Mn as in (b) we still find that the Mn electrons plague the states at E_F in spin down. In analog we see from (b) and (c) that also Cr negatively impacts to the band gap especially in spin up. The sole permutation with clear evidence of a spin down gap is from the chromium poor permutation plotted in (d). Also in this structure we see that the effects of Mn around E_F is dampened in comparison to the other permutations, despite containing relatively increased amounts of Mn to the eqvimolar alloy.

An important property of these results is that because each permutation alters simultaneous elements, interpreting and relating the results to a particular alteration is challenging. For example, is the result of the $Cr_5Fe_3Mn_5Ni_3Si_{32}$ permutation a consequence of less Fe or increments to both Cr and Mn? Furthermore is the large band gap in spin up of $Cr_3Fe_3Mn_7Ni_3Si_{32}$ a product of increasing manganese or reducing the other elements. From the comparatively large gaps in spin up of $Cr_3Fe_3Mn_7Ni_3Si_{32}$ and $Cr_3Fe_5Mn_5Ni_3Si_{32}$ and the more present Cr states in spin up in the Cr rich permutations we here conclude that the band gap is related to lessening of chromium, more so than other effects. However we see from both $Cr_5Fe_5Mn_4Ni_3Si_{32}$ and $Cr_3Fe_3Mn_3Ni_7Si_{32}$ (figure 8.2) in addition to the manganese rich composition that Mn plays a vital role on the band gap of these structures. It's clear that the $Cr_3Fe_5Mn_5Ni_3Si_{32}$ alloy manage to strike a balance between 3d elements that results in a specific interplay and correspondingly very promising properties.

Part IV

Conclusion

Write conclusion here